SEMARAK ILMU PUBLISHING

CFD Letters

Journal homepage:
https://semarakilmu.com.my/journals/index.php/CFD_Letters/index
ISSN: 2180-1363

Influence of Both Ohmic Dissipation and Activation Energy on Peristaltic Transport of Jeffery Nanofluid through a Porous Media

Alaa Abuiyada[1,*], Nabil Eldabe[2], Mohamed Abouzeid[2], Sami Elshaboury[1]

[1] Department of mathematics, Faculty of Science, Ain Shams University, Cairo, Egypt
[2] Department of mathematics, Faculty of Education, Ain Shams University, Cairo, Egypt

ARTICLE INFO

Article history:
Received 5 November 2022
Received in revised form 6 December 2022
Accepted 1 January 2023
Available online 1 June 2023

Keywords:
Peristalsis; MHD Jeffery fluid; activation energy; thermal diffusion and diffusion thermo effects; homotopy perturbation method (HPM)

ABSTRACT

The theme of this study is to investigate the influence of the chemical reaction and activation energy on MHD peristaltic flow of Jeffery nanofluids in an inclined symmetric channel through a porous medium. Joule heating, radiation, viscous dissipation, heat generation/absorption, activation energy, and thermal diffusion and diffusion thermo effects are involved. The long wavelength and low Reynolds number approximations are used to simplify the non-linear equations that govern the flow. Then, the simplified equations are solved by using the homotopy perturbation method (HPM). We have depicted the velocity, temperature, solute concentration, and nanoparticles volume friction graphically. Physical explanations for the results are provided. The influence of interest parameters on entropy generation is also observed. Numerical results for the heat transfer coefficient, Nusselt number, and Sherwood number are presented. The results revealed that an increase in the value of the ratio of relaxation to retardation times of Jeffery nanofluid λ_1 enhances the velocity distribution, while a reduction in the solute concentration distribution occurs by increasing the activation energy parameter E and the temperature difference parameter ρ_1. We also discovered that an increase of the chemical reaction parameter ξ increases the temperature profile and decreases the velocity and solute concentration profiles. Furthermore, the velocity becomes lower along the normal axis y and ends up with the minimum value near the upper wall of the channel. Also, the maximum and minimum values of the velocity increase with an increase of the second order slip parameter β_2, while they decrease as Darcy number Da increases.

1. Introduction

The study of peristalsis attracted the attention of many researchers due to its significant role in the transport processes. Application of peristalsis in the human body occurs in the movement of food

* *Corresponding author.*
E-mail address: alaaabuiyada2019@gmail.com (Alaa Abuiyada)

https://doi.org/10.37934/cfdl.15.6.6585

particles through the digestive tract, the motion of chyme via the gastrointestinal tract, and the transfer of urine from the kidneys to the bladder. Moreover, many devices have been created based on the principle of peristalsis as blood pump machines, dialysis machines, and heart-lung machines. El-dabe *et al.,* [1] studied the peristaltic motion of Eyring-Powell nanofluid with couple stresses and heat and mass transfer through a porous media under the effect of magnetic field inside asymmetric vertical channel. Abbasi *et al.,* [2] studied the slip effects on mixed convective peristaltic transport of copper-water nanofluid in an inclined channel. El-dabe *et al.,* [3] analyzed the peristaltic flow of Herschel Bulkley nanofluid through a non-Darcy porous medium with heat transfer under slip condition. El-dabe *et al.,* [4] investigated MHD peristaltic flow of non-Newtonian power-law nanofluid through a non-Darcy porous medium inside a non-uniform inclined channel. Mansour and Abou-zeid [5] studied the heat and mass transfer effects on Non-Newtonian fluid flow in a non-uniform vertical tube with peristalsis. El-dabe and Abou-zeid [6] studied the radially varying magnetic field effect on peristaltic motion with heat and mass transfer of a non-Newtonian fluid between two co-axial tubes. El-dabe *et al.,* [7] studied a semi-analytical technique for MHD peristalsis of pseudoplastic nanofluid with temperature dependent viscosity. Many researchers have studied different flows with peristalsis [8-12].

Nanofluids are nanometer-sized materials such as aluminium oxide (Al_2O_3), copper (Cu), copper-oxide (CuO), gold (Au), silver (Ag), etc., dispersed in a base fluid such as water, oil, ethylene glycol, polymer solution, and bio-fluids. Gold nanoparticles play a significant role in the biomedical sciences and emerge as promising agents for treatment. The small size of the gold nanoparticles and their ability to penetrate widely over the body made them attractive for application in cancer therapy. Further, they can bind many proteins and drugs and they can also actively target the cancer cells, treat them, and kill the bacteria. Furthermore, the high atomic number of the gold nanoparticles leads to produce heat which can be used for tumor-selective photothermal therapy. Peristaltic flows with gold nanoparticles have been investigated to examine the characteristics of gold nanoparticles in biological flows. El-dabe *et al.,* [13] investigated MHD peristaltic flow of a third grade nanofluid through a porous medium. Mekheimer *et al.,* [14] studied the peristaltic blood flow with gold nanoparticles as a third grade nanofluid in catheter. They pointed out that the gold nanoparticles are effective for drug carrying and drug delivery systems because they control the velocity through the Brownian motion parameter Nb and thermophoresis parameter Nt, also they found that the gold nanoparticles enhance the temperature distribution which assists them to destroy the cancer cells. Simulation of gold nanoparticle transport during MHD electroosmotic flow in a peristaltic micro-channel for biomedical treatment was analyzed by Nuwairan and Souayeh [15]. Asha and Sunitha [16] investigated the influence of thermal radiation on peristaltic blood flow of a Jeffrey fluid with double diffusion in the presence of gold nanoparticles. They found that the impact of thermal radiation on blood flow with gold nanoparticles increases the temperature profile, which helps in destroying cancer cells during the drug delivery process. Umavathi *et al.,* [17] studied the magnetohydrodynamic squeezing Casson nanofluid flow between parallel convectively heated disks.

Newtonian fluids define as the fluids in which the shear stress is linearly proportional to the shear strain rate such as kerosene, gasoline water, air, and other gases. Otherwise, Fluids for which the shear stress is not linearly related to the shear strain rate are called non-Newtonian fluids like ketchup, polymer solutions, paste, paint, and cake batter. Blood exhibits non-Newtonian behavior under low shear stress and Newtonian behavior under high shear stress. Shear stress must be high for blood to flow through big veins and arteries and low for blood to flow through tiny veins and arteries. Jeffery fluid behaves like both Newtonian and non-Newtonian fluids depending on the core and peripheral regions. Many types of researches have been done to study Jeffery fluid in different geometries. Saleem *et al.,* [18] studied the impact of velocity second slip and inclined magnetic field

on peristaltic flow coating with Jeffrey fluid in tapered channel. El-dabe *et al.,* [19] studied a semi-analytical treatment of Hall current effect on peristaltic flow of Jeffery nanofluid. Abd-Alla and Abo-Dahab [20] analyzed the magnetic field and rotation effects on peristaltic transport of a Jeffrey fluid in an asymmetric channel. Abd-Alla *et al.,* [21] obtained a numerical solution for MHD peristaltic transport in an inclined nanofluid symmetric channel with porous medium. They found that an increase in the ratio of relaxation to retardation times of Jeffery fluid λ_1 causes a reduction in the velocity profile at the middle of the channel, while an opposite behavior occurs near the walls of the channel. Rafiq *et al.,* [22] analyzed MHD electroosmotic peristaltic flow of Jeffrey nanofluid with slip conditions and chemical reaction. Hayat *et al.,* [23] studied the radiative peristaltic flow of Jeffrey nanofluid with Slip conditions and Joule heating. El-dabe *et al.,* [24] studied the magnetohydrodynamic peristaltic flow of Jeffry nanofluid with heat transfer through a porous medium in a vertical Tube. Sarada *et al.,* [25] investigated the effect of magnetohydrodynamics on heat transfer behaviour of a non-Newtonian fluid flow over a stretching sheet under local thermal Non-equilibrium condition. Kumar *et al.,* [26] studied non-Newtonian hybrid nanofluid flow over vertically upward/downward moving rotating disk in a Darcy–Forchheimer porous medium. Gowda *et al.,* [27] analyzed the dynamics of nanoparticle diameter and interfacial layer on flow of non-Newtonian (Jeffrey) nanofluid over a convective curved stretching sheet.

The magnetic field with a nonzero inclination is referred to an inclined magnetic field. So, we may declare that the inclined magnetic field is the generalization of a magnetic field. The inclination is required to explain the effectiveness of magnetohydrodynamic (MHD) plasma devices, energy systems, and accelerators as well as for the fulfillment of more real-world geophysical and biological fluxes. The influence of inclined magnetic fields on peristaltic flows has been presented by many researchers. Hayat *et al.,* [28] studied the outcome of slip features on the peristaltic flow of a Prandtl nanofluid with inclined magnetic field and chemical reaction. Kamal and Abdulhadi [29] investigated the influence of an inclined magnetic field on peristaltic transport of pseudoplastic nanofluid through a porous space in an inclined tapered asymmetric channel with convective conditions. Akram *et al.,* [30] studied the effects of heat and mass transfer on peristaltic flow of a Bingham fluid in the presence of inclined magnetic field and channel with different wave forms. Hayat *et al.,* [31] investigated the magnetohydrodynamic effects on peristaltic flow of hyperbolic tangent nanofluid with slip conditions and Joule heating in an inclined channel. They observed that increasing the inclination angle of both channel and magnetic field increases the velocity and temperature profiles, whereas a reduction occurs in the nanoparticle concentration profile. Noreen and Qasim [32] analyzed the peristaltic flow with inclined magnetic field and convective boundary conditions. Gowda *et al.,* [33] studied three-dimensional non-Newtonian magnetic fluid flow induced due to stretching of the flat surface with chemical reaction.

The study of entropy generation determines the energy losses of the engineering and industrials thermal systems. Entropy generation is used in turbomachinery, electronic cooling, porous media, heat exchanger pumps, solar collectors, combustions, and chemical vapour deposition instruments. Various researchers considered entropy generation in their studies. Ouaf *et al.,* [34] analyzed the entropy generation and chemical reaction effects on MHD non-Newtonian nanofluid flow in a sinusoidal channel. Ismael *et al.,* [35] investigated entropy generation and nanoparticles CuO effects on MHD peristaltic transport of micropolar non-Newtonian fluid with velocity and temperature slip conditions. Akbar *et al.,* [36] obtained the thermal radiation and Hall effects in mixed convective peristaltic transport of nanofluid with entropy generation.

Activation energy is defined as the minimum amount of energy that required to start a chemical reaction. Recently, investigation the impact of chemical reaction and activation energy with peristalsis has attracted the attention of many researchers. Hayat *et al.,* [37] studied the activation

energy and non-Darcy resistance in magneto peristalsis of Jeffrey material. Nisar *et al.,* [38] pointed out the significance of activation energy in radiative peristaltic transport of Eyring-Powell nanofluid. Hayat *et al.,* [39] obtained the activation energy and entropy generation in mixed convective peristaltic transport of Sutterby nanofluid. Ellahi *et al.,* [40] studied the peristaltic blood flow of couple stress fluid suspended with nanoparticles under the influence of chemical reaction and activation energy. Hayat *et al.,* [41] studied the nonlinear radiative peristaltic flow of Jeffrey nanofluid with activation energy and modified Darcy's law. Ibrahim *et al.,* [42] studied the activation energy and chemical reaction effects on MHD Bingham nanofluid flow through a non-Darcy porous medium.

Many researches have been done to study the impact of activation energy in different situations. Gowda *et al.,* [43] investigated the impact of binary chemical reaction and activation Energy on heat and mass transfer of marangoni driven boundary layer flow of a non-Newtonian nanofluid. Kumar *et al.,* [44] studied the Exploring the impact of magnetic dipole on the radiative nanofluid flow over a stretching sheet by means of KKL model. Sarada *et al.,* [45] studied the impact of exponential form of internal heat generation on water-based ternary hybrid nanofluid flow by capitalizing non-Fourier heat flux model. Gowda *et al.,* [46] analyzed the KKL correlation for simulation of nanofluid flow over a stretching sheet considering magnetic dipole and chemical reaction. The computational investigation of Stefan Blowing effect on flow of second-grade fluid over a curved stretching sheet was done by Gowda *et al.,* [47]. Exploration of Arrhenius activation energy on hybrid nanofluid flow over a curved stretchable surface was investigated by Kumar *et al.,* [48]. Kumar *et al.,* [49] studied the heat transfer analysis in three-dimensional unsteady magnetic fluid flow of water-based ternary hybrid nanofluid conveying three various shaped nanoparticles. Kumar *et al.,* [50] investigated the inspection of convective heat transfer and KKL correlation for simulation of nanofluid flow over a curved stretching sheet.

From the aforementioned articles, to the best of writer's knowledge that the aspects of chemical reaction and activation energy on MHD peristaltic flow of non-Newtonian Jeffery nanofluid in an inclined symmetric channel through a porous medium was not yet discussed. Hence, the main contribution of this study is to extend the work of Ouaf *et al.,* [34] to examine the flow, heat and mass transfer features of Jeffery nanofluid with chemical reaction and activation energy, radiation, and an inclined magnetic field. The non-linear equations governing the system flow are simplified by using the long wavelength and low Reynolds number approximations. Then, a semi-analytical method called the Homotopy perturbation method (HPM) is used to solve the simplified equations. The influence of Brownian motion and thermophoresis are obtained. Graphs for the solution of velocity, temperature, solutal concentration, and nanoparticles volume friction are plotted to observe the influence of the involved parameters. Further, graphs for the entropy generation are illustrated. Numerical values of the heat transfer coefficient, Nusselt number, and Sherwood number for different values of interest parameters are presented.

2. Mathematical Formulation

Peristaltic flow of MHD Jeffery nanofluid through a porous medium in an inclined symmetric channel having width $2d$ and inclined at an angle α to the horizontal as shown in Figure 1. The Cartesian coordinates are assumed in such a way that the X-axis lies along the centre line of the channel whereas Y-axis is perpendicular to it. The velocity components U and V lie along X and Y directions, respectively. The geometry of the wall surface of a symmetric channel can be described as follows

$$y = \pm h(X,t) = \pm\left[d + a\,cos\frac{2\pi}{\lambda}(X - ct)\right] \tag{1}$$

A magnetic field of strength B_0 is inclined at angle η to the vertical axis of the channel, and may have the following form [31]

$$\boldsymbol{B} = (B_0\ \sin\eta\,, B_0\ \cos\eta\,, 0) \tag{2}$$

By ignoring the Hall and ion-slip effects, the current density $\boldsymbol{J}$ can be expressed as [51]

$$\boldsymbol{J} = \sigma_f(\boldsymbol{E} + \boldsymbol{V} \times \boldsymbol{B}) \tag{3}$$

Here, $\boldsymbol{E}$ is the electric field and assumed to be zero since there is no polarization voltage, σ_f is the electric conductivity of the fluid, and $\boldsymbol{V}$ is the vector velocity. Eq. (3) can be rewritten with the help of Eq. (2) as follows [31]

$$\boldsymbol{J} = \sigma_f\ B_0(U\ \cos\eta - V\sin\eta)\hat{k} \tag{4}$$

The terms $\boldsymbol{J} \times \boldsymbol{B}$, $\frac{\boldsymbol{JJ}}{\sigma_f}$ represent the Lorentz force per unit volume and Joule heating, respectively. These terms can be written by using Eq. (3) and Eq. (4) as follows [31]

$$\boldsymbol{F} = \boldsymbol{J} \times \boldsymbol{B} = \sigma_f\ B_0^2(U\cos\eta - V\sin\eta)(\ \sin\eta\,\hat{\jmath} - \cos\eta\,\hat{\imath}) \tag{5}$$

$$\frac{\boldsymbol{JJ}}{\sigma_f} = \rho_f B_0^2(U^2 cos^2\eta - 2UV\cos\eta\ \sin\eta + V^2 sin^2\eta) \tag{6}$$

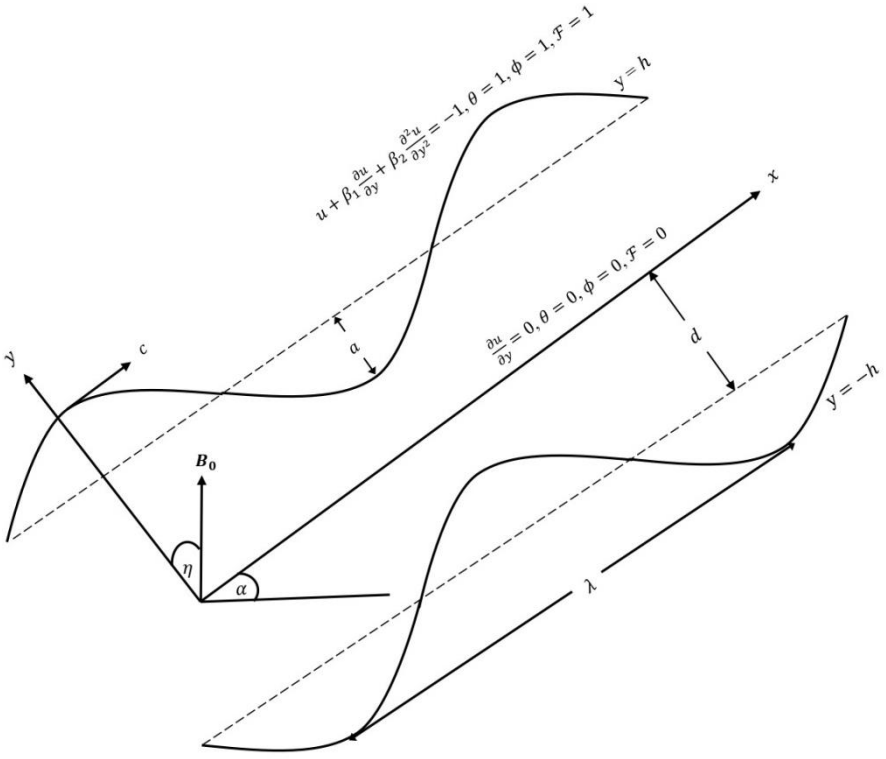

Fig. 1. Geometry of the problem

The governing equations for MHD Jeffery nanofluid in the presence of chemical reaction and activation energy, Joule heating, viscous dissipation, radiation, heat generation/absorption, and thermal diffusion and diffusion thermo effects are described as [52]

$$\frac{\partial U}{\partial X}+\frac{\partial V}{\partial Y}=0 \tag{7}$$

$$\rho_f\left(\frac{\partial U}{\partial t}+U\frac{\partial U}{\partial X}+V\frac{\partial U}{\partial Y}\right)=-\frac{\partial P}{\partial X}+\frac{\mu_f}{1+\lambda_1}\left(\frac{\partial^2 U}{\partial X^2}+\frac{\partial^2 U}{\partial Y^2}\right)+\rho_f g\ sin\,\alpha\left(\beta_T(T-T_0)+\ \beta_C(C-C_0)-\beta_f(f-f_0)\right)-\rho_f B_0^2\ \cos\eta\,(U\cos\eta-V\sin\eta)-\frac{\mu_f}{k_1}U \tag{8}$$

$$\rho_f\left(\frac{\partial V}{\partial t}+U\frac{\partial V}{\partial X}+V\frac{\partial V}{\partial Y}\right)=-\frac{\partial P}{\partial Y}++\frac{\mu_f}{1+\lambda_1}\left(\frac{\partial^2 V}{\partial X^2}+\frac{\partial^2 V}{\partial Y^2}\right)+\rho_f g\ \cos\alpha\ \left(\beta_T(T-T_0)+\ \beta_C(C-C_0)-\beta_f(f-f_0)\right)+\rho_f B_0^2\ \sin\eta\,(U\cos\eta-V\sin\eta)-\frac{\mu_f}{k_1}V \tag{9}$$

$$(\rho c)_f\left(\frac{\partial T}{\partial t}+U\frac{\partial T}{\partial X}+V\frac{\partial T}{\partial Y}\right)=\kappa_f\left(\frac{\partial^2 T}{\partial X^2}+\frac{\partial^2 T}{\partial Y^2}\right)+\frac{\mu_f}{1+\lambda_1}\left(2\left(\frac{\partial U}{\partial X}\right)^2+\left(\frac{\partial V}{\partial Y}\right)^2+\left(\frac{\partial U}{\partial Y}+\frac{\partial V}{\partial X}\right)^2\right)+(\rho c)_p\left[D_B\left(\frac{\partial T}{\partial X}\frac{\partial f}{\partial X}+\frac{\partial T}{\partial Y}\frac{\partial f}{\partial Y}\right)+\frac{D_T}{T_m}\left(\left(\frac{\partial T}{\partial X}\right)^2+\left(\frac{\partial T}{\partial Y}\right)^2\right)\right]+\ D_{TC}\left(\frac{\partial^2 C}{\partial X^2}+\frac{\partial^2 C}{\partial Y^2}\right)+\rho_f B_0^2(U^2 cos^2\eta-2UV\cos\eta\sin\eta+V^2 sin^2\eta)+Q_0(T-T_0)-\frac{\partial q_r}{\partial Y} \tag{10}$$

$$\frac{\partial C}{\partial t}+U\frac{\partial C}{\partial X}+V\frac{\partial C}{\partial Y}\ =D_s\left(\frac{\partial^2 C}{\partial X^2}+\frac{\partial^2 C}{\partial Y^2}\right)+D_{CT}\left(\frac{\partial^2 T}{\partial X^2}+\frac{\partial^2 T}{\partial Y^2}\right)-K_r^2\ (C-C_0)\left(\frac{T}{T_0}\right)exp\left(\frac{E_a}{k\,T}\right) \tag{11}$$

$$\frac{\partial f}{\partial t}+U\frac{\partial f}{\partial X}+V\frac{\partial f}{\partial Y}\ =D_B\left(\frac{\partial^2 f}{\partial X^2}+\frac{\partial^2 f}{\partial Y^2}\right)+\frac{D_T}{T_m}\left(\frac{\partial^2 T}{\partial X^2}+\frac{\partial^2 T}{\partial Y^2}\right) \tag{12}$$

The radiative heat flux q_r is given by [16,23]

$$q_r=\frac{-4\sigma^*}{3k_R}\frac{\partial T^4}{\partial Y} \tag{13}$$

where σ^*, k_R are the Stefan-Boltzmann constant and the mean absorption coefficient, respectively. Here, the difference in temperature within the flow is sufficiently small as the term T^4 in Taylor series about temperature T_0 which can be expressed as follows

$$T^4=T_0^4+4\,T_0^3(T-T_0)+6\,T_0^2\ (T-T_0)^2+\cdots \tag{14}$$

Neglecting the higher order terms of Eq. (14) beyond the first order in $(T-T_0)$, we obtain

$$T^4\cong 4\,T_0^3T-3T_0^4 \tag{15}$$

Substituting Eq. (15) into Eq. (13), we get

$$q_r=-\frac{16\,\sigma^*T_0^3}{3k_R}\frac{\partial T}{\partial Y} \tag{16}$$

Transformation between laboratory and moving frames is given as

$$y = Y,\ x = X - ct,\ p(x,y) = P(X,Y,t), u = U - c, v = V(x,y,t),\ T(x,y) = T(X,Y,t), C(x,y) = C(X,Y,t), f(x,y) = f(X,Y,t) \tag{17}$$

Where (u,v) are the velocity components in the wave frame (x,y). Defining the following non-dimensional quantities

$$u^* = \frac{u}{c}\ , v^* = \frac{v}{c\delta}\ , x^* = \frac{x}{\lambda'}\ y^* = \frac{y}{d}\ , t^* = \frac{ct}{\lambda}, p^* = \frac{d^2p}{c\lambda\mu}\ , \theta = \frac{T-T_0}{T_1-T_0}\ , \phi = \frac{C-C_0}{C_1-C_0}\ , \mathcal{F} = \frac{f-f_0}{f_1-f_0}, Re = \frac{\rho_f cd}{\mu}\ ,$$
$$\delta = \frac{d}{\lambda}\ ,\ M = \sqrt{\frac{\sigma}{\mu}}B_0 d,\ Pr = \frac{\mu c_p}{k}\ ,\ Ec = \frac{c^2}{c_{p(T_1-T_0)}},\ Br = Ec\ Pr,\ \epsilon = \frac{a}{d},\ Da = \frac{k_1}{d^2},\ R = \frac{4\sigma^* T_0^3}{k_f k_R},\ Nb =$$
$$\frac{\tau_1 D_B}{\nu}(f_1 - f_0), Nt = \frac{\tau_1 D_T}{\nu\, T_m}(T_1 - T_0),\ N_{TC} = \frac{D_{TC}\,(C_1-C_0)}{\mu_f c_p (T_1-T_0)},\ N_{CT} = \frac{D_{CT}\,(T_1-T_0)}{D_s\,(C_1-C_0)},\ \rho_1 = \frac{T_1-T_0}{T_0},\ E = \frac{E_a}{K\,T_0},\ \xi =$$
$$\frac{K_r^2\, d^2}{D_s}\, Gr = \frac{\rho_f g \beta_T\, d^2 (T_1-T_0)}{c\mu_f},\ Gc = \frac{\rho_f g \beta_C d^2 (C_1-C_0)}{c\mu_f},\ Gc = \frac{\rho_f g \beta_f d^2 (f_1-f_0)}{c\mu_f},\ Q = \frac{Q_0\, d^2}{\mu_f c_p} \tag{18}$$

By applying the transformation between laboratory and moving frames in Eq. (17) and using the above non-dimensional parameters defined in Eq. (18). Eq. (8) to Eq. (12) can be written after applying the low Reynolds number and long-wavelength approximation as follows

$$\frac{\partial P}{\partial x} = \frac{1}{1+\lambda_1}\frac{\partial^2 u}{\partial y^2} + (Gr\theta + Gc\phi - Gf\mathcal{F})\sin\alpha - \left(\frac{1}{Da} + M^2 cos^2\eta\right)(u+1) \tag{19}$$

$$\frac{\partial P}{\partial y} = 0 \tag{20}$$

$$\left(1 + \frac{4}{3}R\right)\frac{\partial^2\theta}{\partial y^2} + \frac{Br}{1+\lambda_1}\left(\frac{\partial u}{\partial y}\right)^2 + Nb\ Pr\frac{\partial\theta}{\partial y}\frac{\partial\mathcal{F}}{\partial y} + Nt\ Pr\left(\frac{\partial\theta}{\partial y}\right)^2 + N_{TC}\ Pr\frac{\partial^2\phi}{\partial y^2} + Q\ Pr\ \theta + M^2 Br\ (u+1)^2 cos^2\eta = 0 \tag{21}$$

$$\frac{\partial^2\phi}{\partial y^2} + N_{CT}\frac{\partial^2\theta}{\partial y^2} - \xi\ \phi\ (\rho_1\theta + 1) exp\left(\frac{E}{(\rho_1\theta+1)}\right) = 0 \tag{22}$$

$$\frac{\partial^2\mathcal{F}}{\partial y^2} + \frac{Nt}{Nb}\frac{\partial^2\theta}{\partial y^2} = 0 \tag{23}$$

Dimensionless boundary conditions are given as [34]

$$\frac{\partial u}{\partial y} = 0, \theta = 0, \phi = 0, \mathcal{F} = 0 \qquad \text{at} \quad y = 0 \tag{24}$$

$$u + \beta_1\frac{\partial u}{\partial y} + \beta_2\frac{\partial^2 u}{\partial y^2} = -1, \theta = 1, \phi = 1, \mathcal{F} = 1 \qquad \text{at} \quad y = h \tag{25}$$

3. Method of Solution: Homotopy Perturbation Method (HPM)

The homotopy perturbation method is one of the notable semi-analytical approaches used to solve the nonlinear partial and ordinary differential equations. The homotopy perturbation method recommends to write the equations governing the flow as follows [34,53]

$$(1-p)\left(\frac{1}{1+\lambda_1}\frac{\partial^2 u}{\partial y^2}-\frac{1}{1+\lambda_1}\frac{\partial^2 u_0}{\partial y^2}\right)+p\left(\frac{1}{1+\lambda_1}\frac{\partial^2 u}{\partial y^2}+(Gr\theta+Gc\phi-Gf\mathcal{F})\sin\alpha-\left(\frac{1}{Da}+M^2cos^2\eta\right)(u+1)-\frac{\partial P}{\partial x}\right)=0 \quad (26)$$

$$(1-p)\left(\left(1+\frac{4}{3}R\right)\frac{\partial^2\theta}{\partial y^2}-\left(1+\frac{4}{3}R\right)\frac{\partial^2\theta_0}{\partial y^2}\right)+p\left(\left(1+\frac{4}{3}R\right)\frac{\partial^2\theta}{\partial y^2}+\frac{Br}{1+\lambda_1}\left(\frac{\partial u}{\partial y}\right)^2+Nb\,Pr\frac{\partial\theta}{\partial y}\frac{\partial\mathcal{F}}{\partial y}+Nt\,Pr\left(\frac{\partial\theta}{\partial y}\right)^2+N_{TC}\,Pr\frac{\partial^2\phi}{\partial y^2}+Q\,Pr\,\theta+M^2Br\,(u+1)^2cos^2\eta\right)=0 \quad (27)$$

$$(1-p)\left(\frac{\partial^2\phi}{\partial y^2}-\frac{\partial^2\phi_0}{\partial y^2}\right)+p\left(\frac{\partial^2\phi}{\partial y^2}+N_{CT}\frac{\partial^2\theta}{\partial y^2}-\xi\,\phi\,(\rho_1\theta+1)exp\left(\frac{E}{(\rho_1\theta+1)}\right)\right)=0 \quad (28)$$

$$(1-p)\left(\frac{\partial^2\mathcal{F}}{\partial y^2}-\frac{\partial^2\mathcal{F}_0}{\partial y^2}\right)+p\left(\frac{\partial^2\mathcal{F}}{\partial y^2}+\frac{Nt}{Nb}\frac{\partial^2\theta}{\partial y^2}\right)=0 \quad (29)$$

The initial approximations u_0, θ_0, ϕ_0 and $\mathcal{F}_0$can be written as the following

$$u_0=-1\,,\,\theta_0=\frac{y}{h}\,,\,\phi_0=\frac{y}{h}\,,\,\mathcal{F}_0=\frac{y}{h} \quad (30)$$

The solution of u, θ, ϕ and $\mathcal{F}$ can be expressed in terms of power series form as follows

$$(u,\theta,\phi,\mathcal{F})=(u_0,\theta_0,\phi_0,\mathcal{F}_0)+p\,(u_1,\theta_1,\phi_1,\mathcal{F}_1)+p^2\,(u_2,\theta_2,\phi_2,\mathcal{F}_2)+\cdots \quad (31)$$

where $p\in[0,1]$ is the embedding parameter. Here, we choose $p=1$ to get an accurate approximation for the solution. Therefore, the solution of velocity, temperature, solute concentration, and nanoparticles volume friction may be written as follows:

$$u(x,y)=c_1+c_2y+c_3y^2+c_4y^3+c_5y^4+c_6y^5+c_7\,y^6 \quad (32)$$

$$\theta(x,y)=c_8+c_9y+c_{10}y^2+c_{11}y^3 \quad (33)$$

$$\phi(x,y)=c_{12}+c_{13}\,y+c_{14}y^2+c_{15}\,y^3+c_{16}\,y^4+c_{17}\,y^5+c_{18}\,y^6+c_{19}\,y^7 \quad (34)$$

$$\mathcal{F}(x,y)=c_{20}+c_{21}\,y+c_{22}y^2+c_{23}\,y^3 \quad (35)$$

Here, c_1 - c_{23} are not given here to save space, but they are available upon request. Also, we defined the heat transfer coefficient $Z(x)$, Nusselt number Nu, and Sherwood number Sh at the upper wall of the channel as follows [53-55]

$$Z(x)=\frac{\partial h}{\partial x}\left(\frac{\partial\theta}{\partial y}\right)_{y\to h}\,,\,Nu=-\left(\frac{\partial\theta}{\partial y}\right)_{y\to h}\,,\,Sh=-\left(\frac{\partial\phi}{\partial y}\right)_{y\to h} \quad (36)$$

We obtained the above expressions by substituting Eq. (32) to Eq. (35) into Eq. (36), and then we used the software Mathematica package to evaluate them numerically for different parameters of the given problem.

4. Entropy Generation

The entropy generation equation is modified by involving the effect of Joule heating, radiation, and heat generation/absorption as follows [34,55]

$$Ns = \left(\frac{\partial\theta}{\partial y}\right)^2 + \frac{1}{\left(1+\frac{4}{3}R\right)}\left(\frac{Br}{1+\lambda_1}\left(\frac{\partial u}{\partial y}\right)^2 + Nb\,Pr\frac{\partial\theta}{\partial y}\frac{\partial\mathcal{F}}{\partial y} + Nt\,Pr\left(\frac{\partial\theta}{\partial y}\right)^2 + N_{TC}\,Pr\frac{\partial^2\phi}{\partial y^2} + Q\,Pr\,\theta + M^2Br\,(u+1)^2cos^2\eta\right) \quad (37)$$

5. Results and Discussion

We have examined the impact of the relevant parameters of MHD peristaltic flow of Jeffery nanofluid inside an inclined symmetric channel in the presence of an inclined magnetic field. We obtained the velocity, temperature, solutal concentration and nanoparticles volume friction profiles by considering the following steady values

$dp/dx = 10, \epsilon = t = \beta_1 = \beta_2 = \lambda_1 = \xi = \rho_1 = N_{TC} = N_{CT} = 0.1, x = R = Br = Gf = 0.2, \mathrm{Nt} = \mathrm{Nb} = M = Q = 1, \mathrm{Pr} = Gr = Gc = E = 2, Da = 0.3, \alpha = \frac{\pi}{3}$ and $\eta = \frac{\pi}{4}$.

The variation of the velocity distribution u along the normal axis y for different values of the second order slip parameter β_2 and Darcy number Da is illustrated in Figure 2 and Figure 3, respectively. It is clear from these figures that the velocity u increases with an increase of β_2, while it decreases by increasing Da. Moreover, we observed from these figures that the velocity profile is parabolic. Also, the maximum value of the velocity u is always located at the center of the channel (at $y = 0$). We have observed from these figures that the velocity u for various values of β_2 and Da becomes lower along the normal axis y and ends up with the minimum value near the upper wall of the channel. Note that the maximum and minimum values of the velocity u increase with an increase of β_2, while they decrease as Da increases.

We observed that the influence of the ratio of relaxation to retardation times of Jeffery fluid λ_1 on the velocity distribution is similar to the effect of β_2 that is given in Figure 2. It is worth mentioning that $\lambda_1 = 0$ in the Jeffery model corresponds to Newtonian fluid. Therefore, we can say that Newtonian fluid is a special case of Jeffery fluid. But we noticed that the velocity profile for Newtonian fluid (when $\lambda_1 = 0$) is smaller than the velocity for Jeffery fluid. The figure is not given here to avoid any type of repetition. Further, we noticed that the influence on the velocity profile u for different values of β_1, Nt, Nb, Gf, Q, Pr and M is similar to the result obtained in Figure 2, while the influence of α, η, ξ, R, Gr and Gc is like that shown in Figure 3. But, the velocity curves for R, Nt, Nb, Pr, Q, α and ξ are closer to each other comparing with those in Figure 2 and Figure 3. The velocity profiles are parabolic for different values of the involved parameters that mentioned above which are not presented here to save space. Furthermore, we found that the obtained results in Figure 2 and Figure 3 are in a good agreement with those obtained by Ouaf *et al.,* [34].

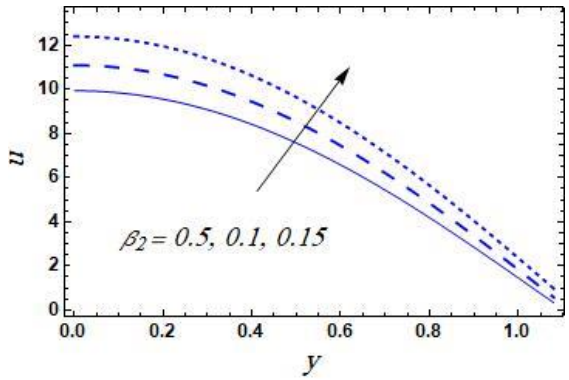

Fig. 2 Variation of β_2 on velocity

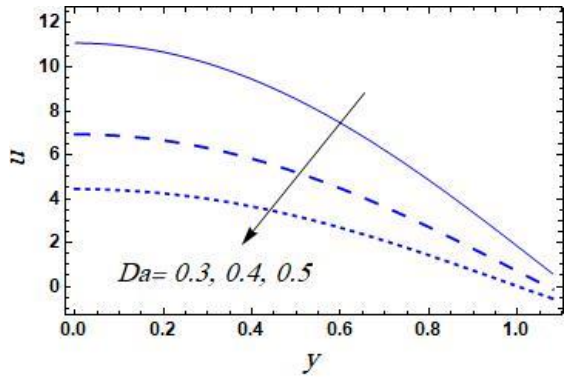

Fig. 3. Variation of Da on velocity

Figure 4 and Figure 5 describe the impact of the chemical reaction parameter ξ and the radiation parameter R on the temperature distribution θ against the normal axis y, respectively. We have observed from these figures that the temperature θ increases as ξ increases, but it decreases by increasing R. Since the thermal radiation is inversely proportional to thermal conduction, the maximum heat of the system radiates away, which reduces the heat conduction of the fluid. It is clear from Figure 4 and Figure 5 that the temperature θ along the normal axis y becomes greater till reaches the maximum value, after which is decreases near the upper wall of the channel. Figure 4 shows that the maximum value of the temperature θ increases by increasing ξ, while it decreases as R increasing. Moreover, the obtained result in Figure 5 is in a good agreement with those obtained by Ouaf *et al.,* [34] and Abuiyada *et al.,* [55]. Furthermore, similar effects on the temperature profile θ as in Figure 4 are observed for Br, Q, Gf and N_{TC}. But the curves captured in Figure 4 are closer to each other than those obtained for Br and Q as captured in Figure 7. Figure 9 shows that the curves obtained for Gf are closer to each other comparing with those in Figure 4. The impact of Gr and Gc on the temperature profile θ is similar to the result in Figure 5, but from Figure 8 we can observe that the resulting curves are closer to each other comparing with those in Figure 5. Some figures are not provided here to avoid any type of repetition. We also observed from Figure 8 and Figure 9 that Gr and Gf affect the temperature distribution θ in an opposite manner. The variation of the temperature distribution θ with the normal axis y for different values of the thermophoresis parameter Nt is depicted in Figure 6. It is revealed from this figure that the temperature θ increases by increasing Nt in the interval ($0 \leq y \leq 0.7$), but an opposite reaction occurs when $y \geq 0.7$. Figure 6 shows that the difference in the temperature profile θ becomes greater and gets to the highest value, after which is decreases and then rises again near the upper wall of the channel. It is clear from this figure that the highest value of the temperature θ increases by increasing the value of Nt. The result in Figure 6 agrees with those obtained by Ouaf *et al.,* [34] and El-dabe *et al.,* [53]. We also observed a similar effect to that captured in Figure 6 for different values of the Brownian motion parameter Nb and Prandtl number Pr. Actually, an improvement in the Brownian motion and thermophoresis effects leads to an active movement of the nanoparticles from the wall to the fluid, which significantly raises the temperature. These figures are omitted here to prevent any kind of duplication.

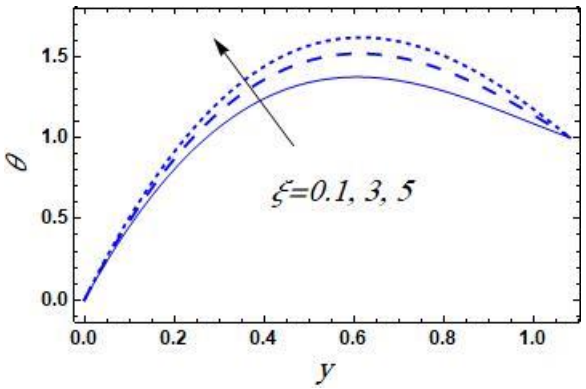

Fig. 4. Variation of ξ on temperature

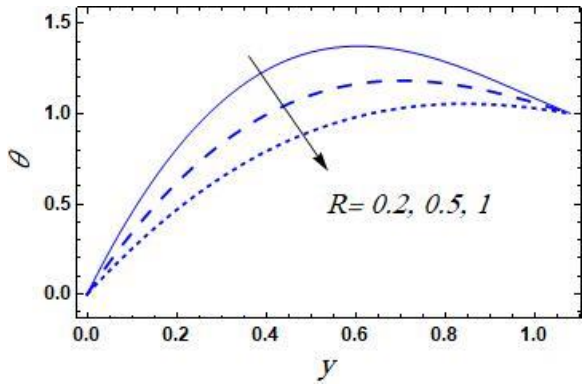

Fig. 5. Variation of R on temperature

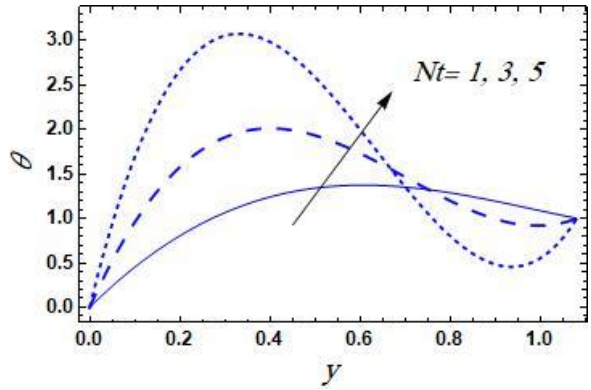

Fig. 6. Variation of Nt on temperature

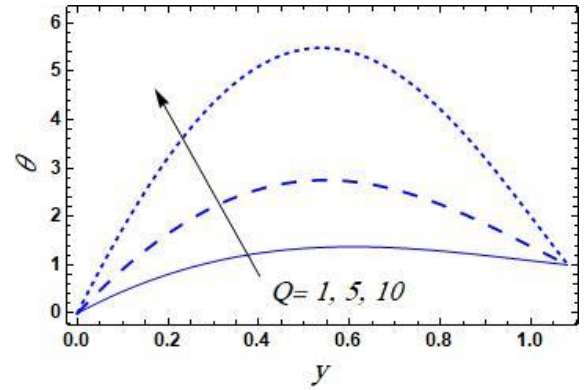

Fig. 7. Variation of Q on temperature

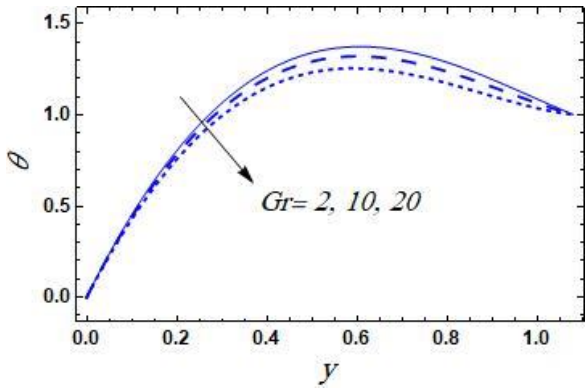

Fig. 8. Variation of Gr on temperature

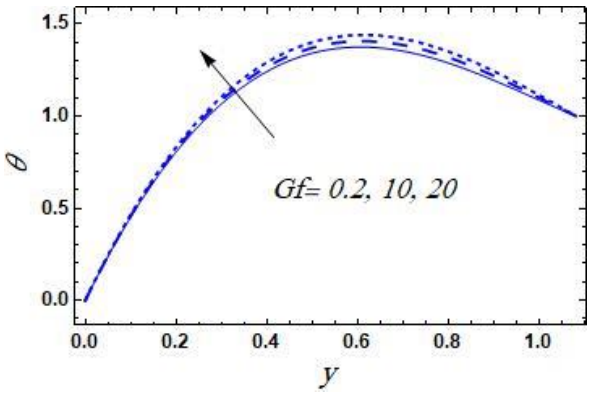

Fig. 9. Variation of Gf on temperature

The variation of the solutal concentration ϕ over the radiation parameter R and the temperature difference parameter ρ_1 against the normal axis y is displayed in Figure 10 and Figure 11, respectively. Figure 10 shows that an increase in R increases the solutal concentration ϕ, while increasing the value of ρ_1 decreases it as seen in Figure 11. In these figures, the variation of the solutal concentration ϕ increases along the normal axis y and ends up with the maximum value at the upper wall of the channel. These figures satisfy the boundary conditions in Eq. (24) and Eq. (25). The influence of Nt, Nb, Q, E, N_{CT}, N_{TC}, ξ and Pr on the solutal concentration ϕ is similar to the effect of $\rho_1$that given in Figure 10. Figure 12 shows that the obtained curves for N_{CT} are not close to each other compared to those curves obtained in Figure 10. It is worth mentioning here that the behavior of the solutal concentration ϕ is similar for both Nt and Nb. Note that some graphs are not given here to save space. Furthermore, it can be noted from the last term of Eq. (22) that the rate of the chemical reaction increases by increasing the value of the chemical reaction parameter ξ which

causes a reduction in the concentration profile as depicted in Figure 13. Note that the activation energy is the minimum energy that required to start the chemical reaction process. Therefore, at a specific value of the activation energy parameter E, the chemical reaction will start which will cause a reduction in the concentration as shown in Figure 14.

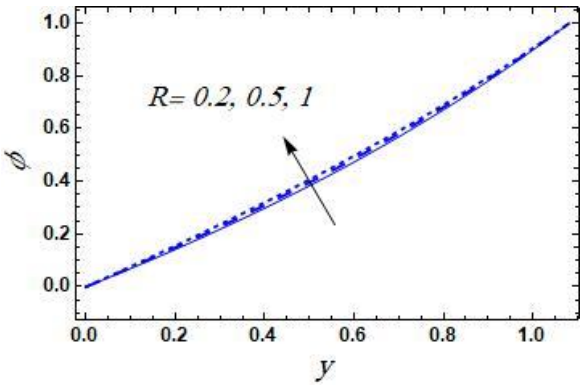

Fig. 10. Variation of R on solutal concentration

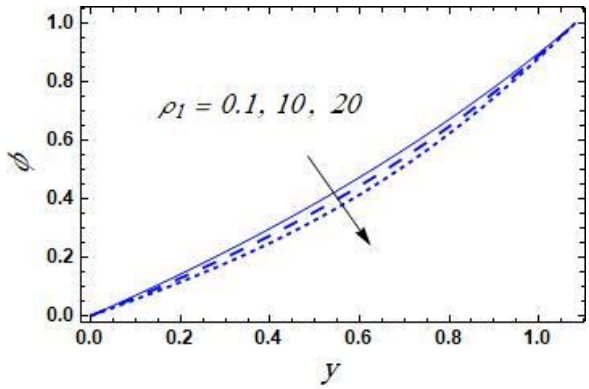

Fig. 11. Variation of ρ_1 on solutal concentration

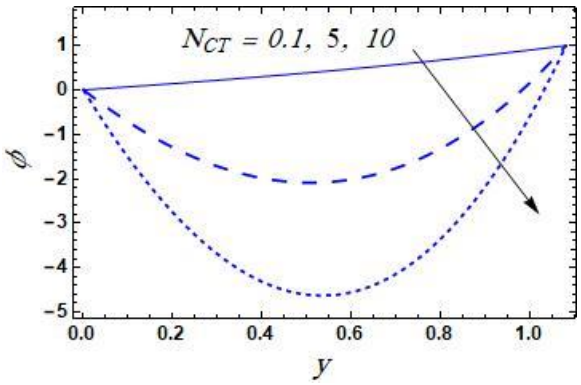

Fig. 12. Variation of N_{CT} on solutal concentration

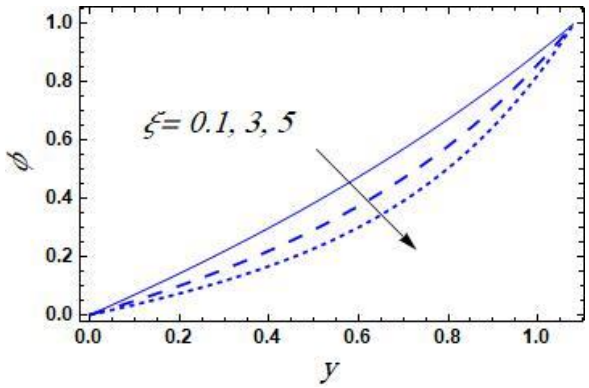

Fig. 13. Variation of ξ on solutal concentration

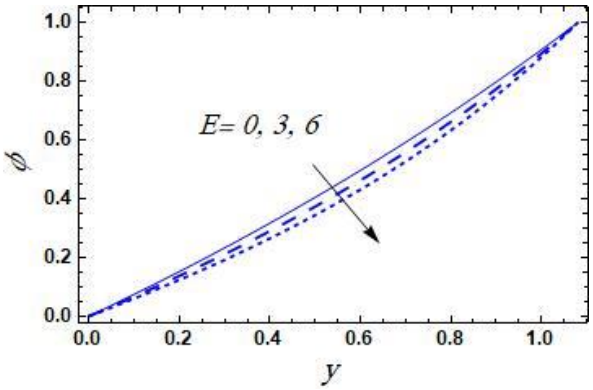

Fig. 14. Variation of E on solutal concentration

Figure 15 and Figure 16 are plotted to observe the effects of various values of the Brownian motion parameter Nb and the thermophoresis parameter Nt on the nanoparticles volume friction profile $\mathcal{F}$ versus the normal axis y. The nanoparticles volume friction $\mathcal{F}$ increases with the increase of Nb as shown in Figure 15. An opposite behavior on the nanoparticles volume friction $\mathcal{F}$ occurs by increasing Nt as shown in Figure 16. It is clear from Figure 15 and Figure 16 that the distribution of nanoparticles volume friction $\mathcal{F}$ becomes lower till reaches the lowest value, after which is increases. The minimum value of the nanoparticles volume friction $\mathcal{F}$ increases by increasing Nb, whereas it

decreases as Nt increases. We found that the results in Figure 15 and Figure 16 are in a good agreement with those obtained by Ouaf *et al.,* [34]. We also observed that the influence of R on the nanoparticles volume friction profile $\mathcal{F}$ along the normal axis y is similar to the effect of Nb that shown in Figure 15, while the influence of Q and Pr on it is very close to the effect of Nt that given in Figure 16. Figure 17 shows the effect of Q on the nanoparticles volume friction profile $\mathcal{F}$. Some figures are not provided here for want of space.

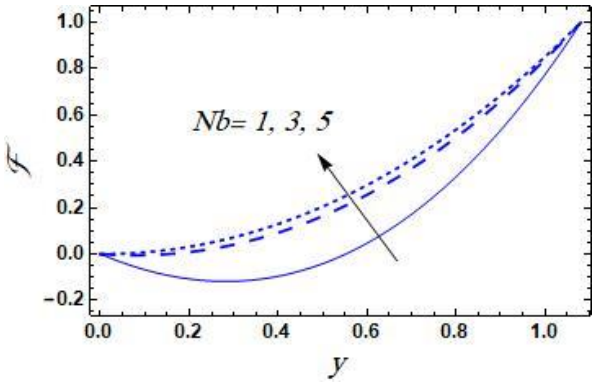

Fig. 15. Variation of Nb on nanoparticles volume friction

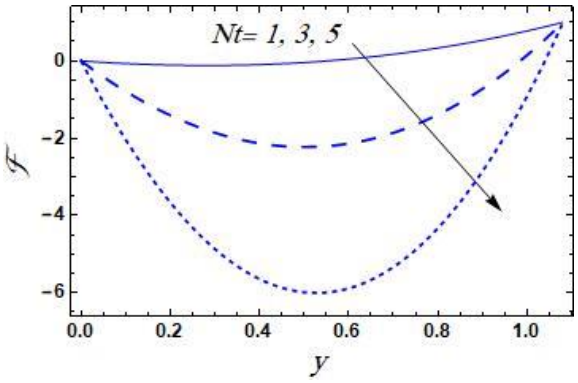

Fig. 16. Variation of Nt on nanoparticles volume friction

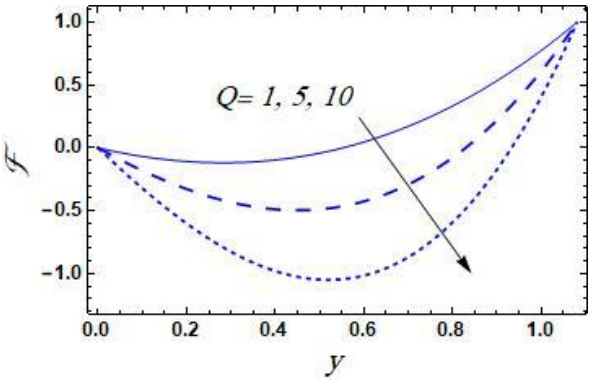

Fig. 17. Variation of Q on nanoparticles volume friction

Figure 18 and Figure 19 are plotted to examine the sequences of the ratio of relaxation to retardation times λ_1 and the inclination angle of the magnetic field parameter η on the entropy generation number Ns along the normal axis y, respectively. We can observe from these figures that the entropy generation number Ns increases by increasing the value of λ_1, while it decreases with an increase of η. Moreover, it is clear from these figures that the variation of the entropy generation number Ns along the normal axis y becomes lower till reaches the minimum value, after which is increases. The minimum value increases by increasing λ_1, while it decreases as η increases. The influence of Br, β_1, β_2, Gf, Q, N_{TC}, N_{CT} and Br is similar to the result captured in Figure 18, and the impact of α and R on it is similar to the effect of η that is illustrated in Figure 19. These figures are not provided here to prevent any kind of duplication. Figure 20 shows that the impact of the local mass Grashof number Gc on the entropy generation number Ns versus the normal axis y is similar to the effect of η captured in Figure 19. But we noticed from Figure 20 that for a large value of Gc the variation of the entropy generation number Ns becomes lower and ends up with the minimum value at the upper wall of the channel. Similar effects to that obtained in Figure 20 can be observed for various values of Da and Gr.

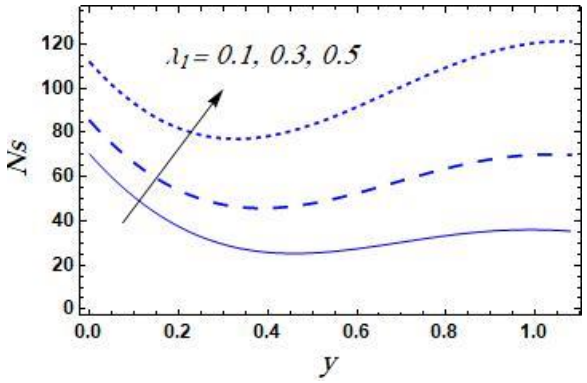

Fig. 18. Variation of λ_1 on entropy generation

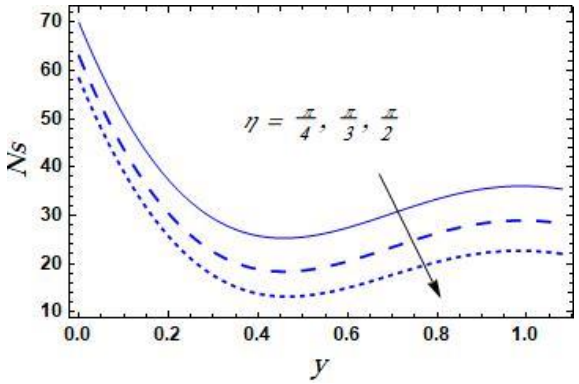

Fig. 19. Variation of η on entropy generation

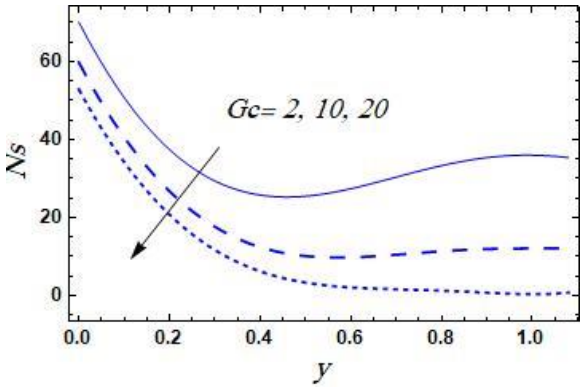

Fig. 20. Variation of Gc on entropy generation

Note that these figures are omitted here to save space. The variation of different values of ξ on the entropy generation number Ns against the normal axis y is depicted in Figure 21. This figure shows that the entropy generation number Ns increases with an increase in ξ approximately when $y \leq 0.35$, but an opposite behavior is observed when $y \geq 0.35$. It is clear from this figure that the variation of the entropy generation number Ns along the normal axis y becomes lower to reach down to the lowest value, after which is increases. Note that the lowest value decreases by increasing the value of ξ as shown in Figure 21. Figure 22 depicts the influence of the thermophoresis parameter Nt on the entropy generation number Ns along the normal axis y. We can observe from Figure 22 that the entropy generation number Ns increases with an increase of Nt. For large values of Nt, the relation between Ns and the normal axis y is a wave with one period and there are two minimum values. These minimum values occur at $y = 0.31$ and $y = 0.91$. The influence of Nb and Pr on Ns is closed to the effect of Nt captured in Figure 22. These graphs are not provided here to save space and avoid any type of duplication.

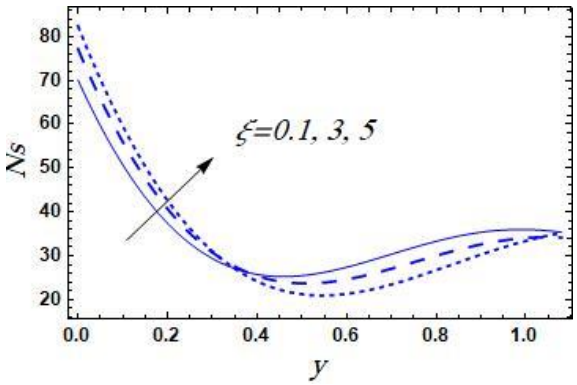

Fig. 21. Variation of ξ on entropy generation

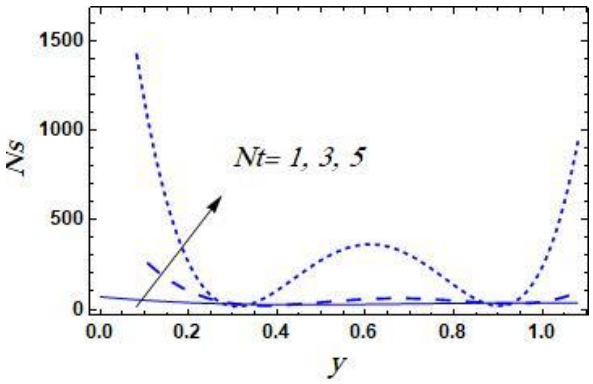

Fig. 22. Variation of Nton entropy generation

Numerical results for heat transfer coefficient, Nusselt number, and Sherwood number are presented in Table 1. It is clear from the table that an increase of R, Nb and Nt decreases the heat transfer coefficient and Nusselt number, while increasing ξ, E, Br, Q and N_{TC} increases them. Moreover, the increase of R, increases the Sherwood number, whereas the increase of ρ_1, ξ, E, Q, N_{CT} and Nb decreases it.

Table 1
Numerical values for heat transfer coefficient, Nusselt number and Sherwood number

R	ρ_1	ξ	E	Q	N_{TC}	N_{CT}	Br	Nb	Nt	$Z(x)$	Nu	Sh
0.2	0.1	0.1	1	1	0.1	0.1	0.2	1	1	0.37030	1.00267	−1.22681
0.5										0.27996	0.75806	−1.17783
1										0.15440	0.41807	−1.13351
	0.5									−	−	−1.25569
	1									−	−	−1.26178
		0.5								0.39341	1.06525	−1.59119
		1								0.42230	1.14347	−1.97828
			2							0.37399	1.01262	−1.28773
			3							0.37765	1.02257	−1.34774
				2						0.61645	1.66918	−1.28398
				3						0.91429	2.47562	−1.34115
					0.5					0.39341	1.06525	−
					1					0.42230	1.14347	−
						0.5				−	−	−2.03868
						1				−	−	−3.05351
							0.5			0.96752	2.61977	−
								2		0.21413	0.57981	−1.30028
									2	−0.04029	−0.10909	−

6. Conclusion

In this study, we have extended the work of Ouaf *et al.,* [34] by considering the influence of the chemical reaction and activation energy on peristaltic flow of MHD Jeffery nanofluid inside an inclined symmetric channel through a porous medium. An inclined magnetic field is applied. The effect of Joule heating, viscous dissipation, radiation, heat generation/absorption, and thermal diffusion and diffusion thermo are taken into account. A semi-analytical method called the homotopy perturbation method (HPM) is employed to solve the equations governing the problem. Graphs for velocity, temperature, solutal concentration, and nanoparticles volume friction distributions are sketched for various values of interest parameters. Numerical results for the heat transfer coefficient, Nusselt number, and Sherwood number are presented. Figures for the influence of interest

parameters on entropy generation number are plotted. Physical explanations for this flow of the obtained results are provided [56-78]. The key findings can be briefed as follows:

(i) The increase of each of β_1, β_2, λ_1, Nt, Nb, Gf, Q, Pr and M increases the velocity, while increasing α, η, ξ, R, Da, Gr and Gc decreases it.

(ii) The velocity u for various values of β_1, β_2, λ_1, Nt, Nb, Gf, Q, Pr, M, α, η, ξ, R, Da, Gr and Gc becomes lower along the normal axis y and ends up with the minimum value near the upper wall of the channel.

(iii) The temperature distribution θ increases as ξ, Br, Q, Gf and N_{TC} increase, but it decreases by increasing R, Gr and Gc.

(iv) The variation of the temperature θ along the normal axis y becomes greater till arrives the maximum value, after which is decreases near the upper wall of the channel.

(v) The temperature distribution θ increases as Nt increases in the interval ($0 \leq y \leq 0.7$), but an opposite reaction occurs when $y \geq 0.7$.

(vi) The difference of the temperature profile θ for different values of Nt becomes greater and gets up to the highest value, after which it decreases and then rises again near the upper wall of the channel.

(vii) The effect of Brownian motion parameter Nb and Prandtl number Pr on the temperature θ is similar to the effect of Nt.

(viii) An increase in R decreases the solutal concentration ϕ, while increasing the value of ρ_1, of Nt, Nb, Q, E, N_{CT}, N_{TC}, ξ and Pr enhances it.

(ix) The variation of the solutal concentration ϕ for various values of R, ρ_1, Nt, Nb, Q, E, N_{CT}, N_{TC}, ξ and Pr increases along the normal axis y and ends up with the maximum value at the upper wall of the channel.

(x) The nanoparticles volume friction $\mathcal{F}$ increases with the increase of Nb and R, but an opposite behavior on the nanoparticles volume friction $\mathcal{F}$ occurs by increasing Nt, Q and Pr.

(xi) The entropy generation number Ns increases by increasing the value of λ_1, Br, β_1, β_2, Gf, Q, N_{TC}, N_{CT} and Br while it decreases with an increase of η, α, Gc, Gr, Da and R.

(xii) The entropy generation number Ns increases with an increase in ξ approximately when $y \leq 0.35$, but an opposite behavior is observed when $y \geq 0.35$.

(xiii) For large values of Nt, the relation between Ns and the normal axis y is a wave with one period and there are two minimum values. These minimum values occur at $y = 0.31$ and $y = 0.91$.

(xiv) An increase of R, Nb and Nt decreases the heat transfer coefficient and Nusselt number, while increasing ξ, E, Br, Q and N_{TC} increases them.

(xv) The increase of R, increases the Sherwood number, whereas the increase of ρ_1, ξ, E, Q, N_{CT} and Nb decreases it.

(xvi) HPM method does not necessitate a small parameter in a system of differential equation.

(xvii) All obtained results show that HPM is an effective method for a highly non-linear systems of differential equations.

(xviii) Heat transfer coefficient, Nusselt number, and Sherwood number results are obtained in accurate solutions using HPM

References

[1] El-dabe, Nabil T., Kawther A. Kamel, Shaimaa F. Ramadan, and Rabab Ahmed Saad. "Peristaltic motion of Eyring-Powell nano fluid with couple stresses and heat and mass transfer through a porous media under the effect of

magnetic field inside asymmetric vertical channel." *Journal of Advanced Research in Fluid Mechanics and Thermal Sciences* 68, no. 2 (2020): 58-71. https://doi.org/10.37934/arfmts.68.2.5871

[2] Abbasi, Fahad Munir, Tasawar Hayat, Bashir Ahmad, and Guo-Qian Chen. "Slip effects on mixed convective peristaltic transport of copper-water nanofluid in an inclined channel." *PLoS One* 9, no. 8 (2014): e105440. https://doi.org/10.1371/journal.pone.0105440

[3] El-dabe, Nabil T., Mohamed Y. Abou-zeid, Mona A. Mohamed, and Mohamed Maged. "Peristaltic flow of Herschel Bulkley nanofluid through a non-Darcy porous medium with heat transfer under slip condition." *International Journal of Applied Electromagnetics and Mechanics* 66, no. 4 (2021): 649-668. https://doi.org/10.3233/JAE-201600

[4] El-dabe, Nabil TM, Mohamed Y. Abou-Zeid, Mona AA Mohamed, and Mohamed M. Abd-Elmoneim. "MHD peristaltic flow of non-Newtonian power-law nanofluid through a non-Darcy porous medium inside a non-uniform inclined channel." *Archive of Applied Mechanics* 91 (2021): 1067-1077. https://doi.org/10.1007/s00419-020-01810-3

[5] Mansour, Hesham Mohamed, and Mohamed Y. Abou-zeid. "Heat and mass transfer effect on non-Newtonian fluid flow in a non-uniform vertical tube with peristalsis." *Journal of Advanced Research in Fluid Mechanics and Thermal Sciences* 61, no. 1 (2019): 44-62.

[6] El-dabe, Nabil, and Mohamed Abou-Zeid. "Radially varying magnetic field effect on peristaltic motion with heat and mass transfer of a non-Newtonian fluid between two co-axial tubes." *Thermal Science* 22, no. 6 Part A (2018): 2449-2458. https://doi.org/10.2298/TSCI160409292E

[7] El-dabe, N. T., G. M. Moatimid, M. Y. Abouzeid, A. A. ElShekhipy, and Naglaa F. Abdallah. "A semianalytical technique for MHD peristalsis of pseudoplastic nanofluid with temperature-dependent viscosity: Application in drug delivery system." *Heat Transfer-Asian Research* 49, no. 1 (2020): 424-440. https://doi.org/10.1002/htj.21619

[8] El-dabe, Nabil T., Mohamed Y. Abou-zeid, Adel Abosaliem, Ahmed Elenna, and Nada Hegazy. "Homotopy perturbation approach for Ohmic dissipation and mixed convection effects on non-Newtonian nanofluid flow between two co-axial tubes with peristalsis." *International Journal of Applied Electromagnetics and Mechanics* 67, no. 2 (2021): 153-163. https://doi.org/10.3233/JAE-210001

[9] El-dabe, Nabil, Mohamed Y. Abou-Zeid, Mahmoud E. Oauf, Doaa R. Mostapha, and Yasmeen M. Mohamed. "Cattaneo-Christov heat flux effect on MHD peristaltic transport of Bingham Al_2O_3 nanofluid through a non-Darcy porous medium." *International Journal of Applied Electromagnetics and Mechanics* 68, no. 1 (2022): 59-84. https://doi.org/10.3233/JAE-210057

[10] Abou-Zeid, M. Y. "Homotopy perturbation method to gliding motion of bacteria on a layer of power-law nanoslime with heat transfer." *Journal of Computational and Theoretical Nanoscience* 12, no. 10 (2015): 3605-3614. https://doi.org/10.1166/jctn.2015.4246

[11] Abou-Zeid, Mohamed Y. "Homotopy perturbation method for couple stresses effect on MHD peristaltic flow of a non-Newtonian nanofluid." *Microsystem Technologies* 24, no. 12 (2018): 4839-4846. https://doi.org/10.1007/s00542-018-3895-1

[12] Ismael, Aya M., Nabil T. Eldabe, Mohamed Y. Abou Zeid, and Sami M. El Shabouri. "Thermal micropolar and couple stresses effects on peristaltic flow of biviscosity nanofluid through a porous medium." *Scientific Reports* 12, no. 1 (2022): 16180. https://doi.org/10.1038/s41598-022-20320-6

[13] El-dabe, N. T., M. Y. Abou-zeid, AS Abo Seliem, A. A. Elenna, and N. Hegazy. "Thermal diffusion and diffusion thermo effects on magnetohydrodynamics transport of non-Newtonian nanofluid through a porous media between two wavy co-axial tubes." *IEEE Transactions on Plasma Science* 50, no. 5 (2022): 1282-1290. https://doi.org/10.1109/TPS.2022.3161740

[14] Mekheimer, Kh S., W. M. Hasona, R. E. Abo-Elkhair, and A. Z. Zaher. "Peristaltic blood flow with gold nanoparticles as a third grade nanofluid in catheter: Application of cancer therapy." *Physics Letters A* 382, no. 2-3 (2018): 85-93. https://doi.org/10.1016/j.physleta.2017.10.042

[15] Nuwairan, Muneerah Al, and Basma Souayeh. "Simulation of gold nanoparticle transport during MHD electroosmotic flow in a peristaltic micro-channel for biomedical treatment." *Micromachines* 13, no. 3 (2022): 374. https://doi.org/10.3390/mi13030374

[16] Asha, S. K., and G. Sunitha. "Influence of thermal radiation on peristaltic blood flow of a Jeffrey fluid with double diffusion in the presence of gold nanoparticles." *Informatics in Medicine Unlocked* 17 (2019): 100272. https://doi.org/10.1016/j.imu.2019.100272

[17] Umavathi, J. C., D. G. Prakasha, Yousef M. Alanazi, Maha MA Lashin, Fahad S. Al-Mubaddel, Raman Kumar, and RJ Punith Gowda. "Magnetohydrodynamic squeezing Casson nanofluid flow between parallel convectively heated disks." *International Journal of Modern Physics B* 37, no. 04 (2023): 2350031. https://doi.org/10.1142/S0217979223500315

[18] Saleem, Najma, Safia Akram, Farkhanda Afzal, Emad H. Aly, and Anwar Hussain. "Impact of velocity second slip and inclined magnetic field on peristaltic flow coating with Jeffrey fluid in tapered channel." *Coatings* 10, no. 1 (2020): 30. https://doi.org/10.3390/coatings10010030

[19] El-dabe, Nabil Tawfik, Galal M. Moatimid, Mohamed Abouzeid, Abdelhafeez A. Elshekhipy, and Naglaa Fawzy Abdallah. "Semi-analytical treatment of Hall current effect on peristaltic flow of Jeffery nanofluid." *International Journal of Applied Electromagnetics and Mechanics* 67, no. 1 (2021): 47-66. https://doi.org/10.3233/JAE-201626

[20] Abd-Alla, A. M., and S. M. Abo-Dahab. "Magnetic field and rotation effects on peristaltic transport of a Jeffrey fluid in an asymmetric channel." *Journal of Magnetism and Magnetic Materials* 374 (2015): 680-689. https://doi.org/10.1016/j.jmmm.2014.08.091

[21] Abd-Alla, A. M., Esraa N. Thabet, and F. S. Bayones. "Numerical solution for MHD peristaltic transport in an inclined nanofluid symmetric channel with porous medium." *Scientific Reports* 12, no. 1 (2022): 3348. https://doi.org/10.1038/s41598-022-07193-5

[22] Rafiq, Maimona, Mehmoona Sajid, Sharifa E. Alhazmi, M. Ijaz Khan, and Essam Rashdy El-Zahar. "MHD electroosmotic peristaltic flow of Jeffrey nanofluid with slip conditions and chemical reaction." *Alexandria Engineering Journal* 61, no. 12 (2022): 9977-9992. https://doi.org/10.1016/j.aej.2022.03.035

[23] Hayat, Tasawar, Maryam Shafique, Anum Tanveer, and Ahmed Alsaedi. "Radiative peristaltic flow of Jeffrey nanofluid with slip conditions and Joule heating." *PloS One* 11, no. 2 (2016): e0148002. https://doi.org/10.1371/journal.pone.0148002

[24] El-dabe, Nabil TM, Mohamed Y. Abou-zeid, and Yasmeen M. Younis. "Magnetohydrodynamic peristaltic flow of Jeffry nanofluid with heat transfer through a porous medium in a vertical tube." *Applied Mathematics & Information Sciences* 11, no. 4 (2017): 1097-1103. https://doi.org/10.18576/amis/110416

[25] Sarada, Konduru, Ramanahalli J. Punith Gowda, Ioannis E. Sarris, Rangaswamy Naveen Kumar, and Ballajja C. Prasannakumara. "Effect of magnetohydrodynamics on heat transfer behaviour of a non-Newtonian fluid flow over a stretching sheet under local thermal non-equilibrium condition." *Fluids* 6, no. 8 (2021): 264. https://doi.org/10.3390/fluids6080264

[26] Kumar, R. Naveen, RJ Punith Gowda, B. J. Gireesha, and B. C. Prasannakumara. "Non-Newtonian hybrid nanofluid flow over vertically upward/downward moving rotating disk in a Darcy-Forchheimer porous medium." *The European Physical Journal Special Topics* 230 (2021): 1227-1237. https://doi.org/10.1140/epjs/s11734-021-00054-8

[27] Gowda, RJ Punith, R. Naveen Kumar, Umair Khan, B. C. Prasannakumara, Aurang Zaib, Anuar Ishak, and Ahmed M. Galal. "Dynamics of nanoparticle diameter and interfacial layer on flow of non-Newtonian (Jeffrey) nanofluid over a convective curved stretching sheet." *International Journal of Modern Physics B* 36, no. 31 (2022): 2250224. https://doi.org/10.1142/S0217979222502241

[28] Hayat, Tasawar, Sabia Asghar, Anum Tanveer, and Ahmed Alsaedi. "Outcome of slip features on the peristaltic flow of a Prandtl nanofluid with inclined magnetic field and chemical reaction." *The European Physical Journal Plus* 132 (2017): 1-16. https://doi.org/10.1140/epjp/i2017-11486-8

[29] Kamal, Ali M., and Ahmed M. Abdulhadi. "Influence of an Inclined Magnetic Field on Peristaltic Transport of Pseudoplastic Nanofluid Through a Porous Space in an Inclined Tapered Asymmetric Channel with Convective Conditions." Am*erican Journal of Mechanics and Applications* 3, no. 5 (2016): 42-55.

[30] Akram, Safia, S. Nadeem, and Anwar Hussain. "Effects of heat and mass transfer on peristaltic flow of a Bingham fluid in the presence of inclined magnetic field and channel with different wave forms." *Journal of Magnetism and Magnetic Materials* 362 (2014): 184-192. https://doi.org/10.1016/j.jmmm.2014.02.063

[31] Hayat, T., Maryam Shafique, Anum Tanveer, and A. Alsaedi. "Magnetohydrodynamic effects on peristaltic flow of hyperbolic tangent nanofluid with slip conditions and Joule heating in an inclined channel." *International Journal of Heat and Mass Transfer* 102 (2016): 54-63. https://doi.org/10.1016/j.ijheatmasstransfer.2016.05.105

[32] Noreen, S., and M. Qasim. "Peristaltic flow with inclined magnetic field and convective boundary conditions." *Applied Bionics and Biomechanics* 11, no. 1-2 (2014): 61-67. https://doi.org/10.1155/2014/426217

[33] Gowda, R. J. Punith, Ioannis E. Sarris, R. Naveen Kumar, Raman Kumar, and B. C. Prasannakumara. "A three-dimensional non-Newtonian magnetic fluid flow induced due to stretching of the flat surface with chemical reaction." *Journal of Heat Transfer* 144, no. 11 (2022): 113602. https://doi.org/10.1115/1.4055373

[34] Ouaf, Mahmoud E., Mohamed Abou-zeid, and Yasmeen M. Younis. "Entropy generation and chemical reaction effects on MHD non-Newtonian nanofluid flow in a sinusoidal channel." *International Journal of Applied Electromagnetics and Mechanics* 69, no. 1 (2022): 45-65. https://doi.org/10.3233/JAE-210215

[35] Ismael, Aya, Nabil Tawfik Eldabe, Mohamed Abouzeid, and Sami Elshabouri. "Entropy generation and nanoparticles Cu O effects on MHD peristaltic transport of micropolar non-Newtonian fluid with velocity and temperature slip conditions." *Egyptian Journal of Chemistry* 65, no. 9 (2022): 715-722.

[36] Akbar, Y., F. M. Abbasi, and S. A. Shehzad. "Thermal radiation and Hall effects in mixed convective peristaltic transport of nanofluid with entropy generation." *Applied Nanoscience* 10 (2020): 5421-5433. https://doi.org/10.1007/s13204-020-01446-3

[37] Hayat, T., A. A. Khan, Farhat Bibi, and S. Farooq. "Activation energy and non-Darcy resistance in magneto peristalsis of Jeffrey material." *Journal of Physics and Chemistry of Solids* 129 (2019): 155-161. https://doi.org/10.1016/j.jpcs.2018.12.044

[38] Nisar, Z., T. Hayat, A. Alsaedi, and B. Ahmad. "Significance of activation energy in radiative peristaltic transport of Eyring-Powell nanofluid." *International Communications in Heat and Mass Transfer* 116 (2020): 104655. https://doi.org/10.1016/j.icheatmasstransfer.2020.104655

[39] Hayat, T., Z. Nisar, A. Alsaedi, and B. Ahmad. "Analysis of activation energy and entropy generation in mixed convective peristaltic transport of Sutterby nanofluid." *Journal of Thermal Analysis and Calorimetry* 143 (2021): 1867-1880. https://doi.org/10.1007/s10973-020-09969-1

[40] Ellahi, Rahmat, Ahmed Zeeshan, Farooq Hussain, and Arash Asadollahi. "Peristaltic blood flow of couple stress fluid suspended with nanoparticles under the influence of chemical reaction and activation energy." *Symmetry* 11, no. 2 (2019): 276. https://doi.org/10.3390/sym11020276

[41] Hayat, T., Farhat Bibi, S. Farooq, and A. A. Khan. "Nonlinear radiative peristaltic flow of Jeffrey nanofluid with activation energy and modified Darcy's law." *Journal of the Brazilian Society of Mechanical Sciences and Engineering* 41 (2019): 1-11. https://doi.org/10.1007/s40430-019-1771-2

[42] Ibrahim, Mohamed, Naglaa Abdallah, and Mohamed Abouzeid. "Activation energy and chemical reaction effects on MHD Bingham nanofluid flow through a non-Darcy porous media." *Egyptian Journal of Chemistry* 65, no. 132 (2022): 137-144.

[43] Gowda, Ramanahalli Jayadevamurthy Punith, Rangaswamy Naveen Kumar, Anigere Marikempaiah Jyothi, Ballajja Chandrappa Prasannakumara, and Ioannis E. Sarris. "Impact of binary chemical reaction and activation energy on heat and mass transfer of marangoni driven boundary layer flow of a non-Newtonian nanofluid." *Processes* 9, no. 4 (2021): 702. https://doi.org/10.3390/pr9040702

[44] Kumar, R. Naveen, S. Suresha, RJ Punith Gowda, Savita B. Megalamani, and B. C. Prasannakumara. "Exploring the impact of magnetic dipole on the radiative nanofluid flow over a stretching sheet by means of KKL model." *Pramana* 95, no. 4 (2021): 180. https://doi.org/10.1007/s12043-021-02212-y

[45] Sarada, K., Fehmi Gamaoun, Amal Abdulrahman, S. O. Paramesh, Raman Kumar, G. D. Prasanna, and RJ Punith Gowda. "Impact of exponential form of internal heat generation on water-based ternary hybrid nanofluid flow by capitalizing non-Fourier heat flux model." *Case Studies in Thermal Engineering* 38 (2022): 102332. https://doi.org/10.1016/j.csite.2022.102332

[46] Gowda, R. J. Punith, R. Naveen Kumar, A. M. Jyothi, B. C. Prasannakumara, and Kottakkaran Sooppy Nisar. "KKL correlation for simulation of nanofluid flow over a stretching sheet considering magnetic dipole and chemical reaction." *ZAMM-Journal of Applied Mathematics and Mechanics/Zeitschrift für Angewandte Mathematik und Mechanik* 101, no. 11 (2021): e202000372. https://doi.org/10.1002/zamm.202000372

[47] Gowda, R. J. Punith, Haci Mehmet Baskonus, R. Naveen Kumar, B. C. Prasannakumara, and D. G. Prakasha. "Computational investigation of Stefan blowing effect on flow of second-grade fluid over a curved stretching sheet." *International Journal of Applied and Computational Mathematics* 7, no. 3 (2021): 109. https://doi.org/10.1007/s40819-021-01041-2

[48] Kumar, R. S. Varun, A. Alhadhrami, R. J. Punith Gowda, R. Naveen Kumar, and B. C. Prasannakumara. "Exploration of Arrhenius activation energy on hybrid nanofluid flow over a curved stretchable surface." *ZAMM-Journal of Applied Mathematics and Mechanics/Zeitschrift für Angewandte Mathematik und Mechanik* 101, no. 12 (2021): e202100035. https://doi.org/10.1002/zamm.202100035

[49] Kumar, R. Naveen, Fehmi Gamaoun, Amal Abdulrahman, Jasgurpreet Singh Chohan, and RJ Punith Gowda. "Heat transfer analysis in three-dimensional unsteady magnetic fluid flow of water-based ternary hybrid nanofluid conveying three various shaped nanoparticles: A comparative study." *International Journal of Modern Physics B* 36, no. 25 (2022): 2250170. https://doi.org/10.1142/S0217979222501703

[50] Kumar, R. Naveen, RJ Punith Gowda, Mohammad Mahtab Alam, Irfan Ahmad, Y. M. Mahrous, M. R. Gorji, and B. C. Prasannakumara. "Inspection of convective heat transfer and KKL correlation for simulation of nanofluid flow over a curved stretching sheet." *International Communications in Heat and Mass Transfer* 126 (2021): 105445. https://doi.org/10.1016/j.icheatmasstransfer.2021.105445

[51] Mohamed, Yasmeen Mostafa, Nabil Tafik El-Dabe, Mohamed Yahya Abou-Zeid, Mahmoud Elhassan Oauf, and Doaa Roshhdy Mostapha. "Peristaltic Transport of Carreau Coupled Stress Nanofluid with Cattaneo-Christov Heat Flux Model Inside a Symmetric Channel: Peristaltic transport of Carreau coupled stress nanofluid." *Journal of Advanced Research in Fluid Mechanics and Thermal Sciences* 98, no. 1 (2022): 1-17. https://doi.org/10.37934/arfmts.98.1.117

[52] El-dabe, Nabil, Abeer A. Shaaban, Mohamed Y. Abou-Zeid, and Hemat A. Ali. "Magnetohydrodynamic non-Newtonian nanofluid flow over a stretching sheet through a non-Darcy porous medium with radiation and chemical reaction." *Journal of Computational and Theoretical Nanoscience* 12, no. 12 (2015): 5363-5371. https://doi.org/10.1166/jctn.2015.4528

[53] El-dabe, Nabil Tawfik, Samy M. El Shaboury, Hassan A. El Arabawy, Mohamed Y. Abou-zeid, and Alaa Abuiyada. "Wall properties and Joule heating effects on MHD peristaltic transport of Bingham non-Newtonian nanofluid." *International Journal of Applied Electromagnetics and Mechanics* 69, no. 1 (2022): 87-106. https://doi.org/10.3233/JAE-210126

[54] Abou-zeid, Mohamed Y., and Mahmoud E. Ouaf. "Hall currents effect on squeezing flow of non-Newtonian nanofluid through a porous medium between two parallel plates." *Case Studies in Thermal Engineering* 28 (2021): 101362. https://doi.org/10.1016/j.csite.2021.101362

[55] Abuiyada, Alaa Jaber, Nabil Tawfik Eldabe, Mohamed Yahya Abou-zeid, and Sami Mohamed El Shaboury. "Effects of Thermal Diffusion and Diffusion Thermo on a Chemically Reacting MHD Peristaltic Transport of Bingham Plastic Nanofluid." *Journal of Advanced Research in Fluid Mechanics and Thermal Sciences* 98, no. 2 (2022): 24-43. https://doi.org/10.37934/arfmts.98.2.2443

[56] Abou-zeid, Mohamed Y. "Magnetohydrodynamic boundary layer heat transfer to a stretching sheet including viscous dissipation and internal heat generation in a porous medium." *Journal of Porous Media* 14, no. 11 (2011): 1007-1018. https://doi.org/10.1615/JPorMedia.v14.i11.50

[57] El-dabe, Nabil T., Sami M. El Shabouri, Tarek N. Salama, and Aya M. Ismael. "Ohmic and viscous dissipation effects on micropolar non-Newtonian nanofluid Al_2O_3 flow through a non-Darcy porous media." *International Journal of Applied Electromagnetics and Mechanics* 68, no. 2 (2022): 209-221. https://doi.org/10.3233/JAE-210100

[58] Mohamed, Mona AA, and Mohamed Y. Abou-zeid. "MHD peristaltic flow of micropolar Casson nanofluid through a porous medium between two co-axial tubes." *Journal of Porous Media* 22, no. 9 (2019): 1079-1093. https://doi.org/10.1615/JPorMedia.2018025180

[59] El-dabe, Nabil Tawfik, Galal M. Moatimid, Mohamed Abouzeid, Abdelhafeez A. El-Shekhipy, and Naglaa Fawzy Abdallah. "Instantaneous thermal-diffusion and diffusion-thermo effects on Carreau nanofluid flow over a stretching porous sheet." *Journal of Advanced Research in Fluid Mechanics and Thermal Sciences* 72, no. 2 (2020): 142-157. https://doi.org/10.37934/arfmts.72.2.142157

[60] El-dabe, Nabil T., Mohamed Y. Abou-Zeid, Omar H. El-Kalaawy, Salah M. Moawad, and Ola S. Ahmed. "Electromagnetic steady motion of Casson fluid with heat and mass transfer through porous medium past a shrinking surface." *Thermal Science* 25, no. 1 Part A (2021): 257-265. https://doi.org/10.2298/TSCI190418416E

[61] El-dabe, Nabil T., Raafat R. Rizkalla, Mohamed Y. Abouzeid, and Vivian M. Ayad. "Thermal diffusion and diffusion thermo effects of Eyring-Powell nanofluid flow with gyrotactic microorganisms through the boundary layer." *Heat Transfer-Asian Research* 49, no. 1 (2020): 383-405. https://doi.org/10.1002/htj.21617

[62] El-dabe, Nabil T., Raafat R. Rizkalla, Mohamed Y. Abou-Zeid, and Vivian M. Ayad. "Effect of induced magnetic field on non-Newtonian nanofluid Al2O3 motion through boundary-layer with gyrotactic microorganisms." *Thermal Science* 26, no. 1 Part B (2022): 411-422. https://doi.org/10.2298/TSCI200408189E

[63] Abou-Zeid, Mohamed Y., Abeer A. Shaaban, and Muneer Y. Alnour. "Numerical treatment and global error estimation of natural convective effects on gliding motion of bacteria on a power-law nanoslime through a non-Darcy porous medium." *Journal of Porous Media* 18, no. 11 (2015): 1091-1106. https://doi.org/10.1615/JPorMedia.2015012459

[64] Abou-zeid, Mohamed Y., and Mona AA Mohamed. "Homotopy perturbation method for creeping flow of non-Newtonian power-law nanofluid in a nonuniform inclined channel with peristalsis." *Zeitschrift für Naturforschung A* 72, no. 10 (2017): 899-907. https://doi.org/10.1515/zna-2017-0154

[65] Abou-Zeid, Mohamed. "Effects of thermal-diffusion and viscous dissipation on peristaltic flow of micropolar non-Newtonian nanofluid: application of homotopy perturbation method." *Results in Physics* 6 (2016): 481-495. https://doi.org/10.1016/j.rinp.2016.08.006

[66] Abou-Zeid, Mohamed. "Homotopy perturbation method to MHD non-Newtonian nanofluid flow through a porous medium in eccentric annuli with peristalsis." *Thermal Science* 21, no. 5 (2017): 2069-2080. https://doi.org/10.2298/TSCI150215079A

[67] Abou-Zeid, Mohamed Y. "Implicit homotopy perturbation method for mhd non-Newtonian nanofluid flow with Cattaneo-Christov heat flux due to parallel rotating disks." *Journal of Nanofluids* 8, no. 8 (2019): 1648-1653. https://doi.org/10.1166/jon.2019.1717

[68] El-dabe, Nabil T., and Mohamed Y. Abou-zeid. "Magnetohydrodynamic peristaltic flow with heat and mass transfer of micropolar biviscosity fluid through a porous medium between two co-axial tubes." *Arabian Journal for Science and Engineering* 39 (2014): 5045-5062. https://doi.org/10.1007/s13369-014-1039-1

[69] El-dabe, Nabil Tawfik, Mohamed Yahya Abou-zeid, and Ola S. Ahmed. "Motion of a thin film of a fourth grade nanofluid with heat transfer down a vertical cylinder: Homotopy perturbation method application." *Journal of Advanced Research in Fluid Mechanics and Thermal Sciences* 66, no. 2 (2020): 101-113.

[70] El-dabe, Nabil, Mohamed Abouzeid, and Hemat A. Ali. "Effect of heat and mass transfer on Casson fluid flow between two co-axial tubes with peristalsis." *Journal of Advanced Research in Fluid Mechanics and Thermal Sciences* 76, no. 1 (2020): 54-75. https://doi.org/arfmts.76.1.5475

[71] El-dabe, Nabil TM, Mohamed A. Hassan, and Mohamed Y. Abou-Zeid. "Wall properties effect on the peristaltic motion of a coupled stress fluid with heat and mass transfer through a porous medium." *Journal of Engineering Mechanics* 142, no. 3 (2016): 04015102. https://doi.org/10.1061/(ASCE)EM.1943-7889.0001029

[72] El-dabe, Nabil Tawfik, Mohamed Abouzeid, and Hamida A. Shawky. "MHD peristaltic transport of Bingham blood fluid with heat and mass transfer through a non-uniform channel." *Journal of Advanced Research in Fluid Mechanics and Thermal Sciences* 77, no. 2 (2021): 145-159. https://doi.org/10.37934/arfmts.77.2.145159

[73] Jamali, Muhammad Sabaruddin Ahmad, Zuhaila Ismail, and Norsarahaida Saidina Amin. "Effect of Different Types of Stenosis on Generalized Power Law Model of Blood Flow in a Bifurcated Artery." *Journal of Advanced Research in Fluid Mechanics and Thermal Sciences* 87, no. 3 (2021): 172-183. https://doi.org/10.37934/arfmts.87.3.172183

[74] ZainulAbidin, Siti Nurulaifa Mohd, Zuhaila Ismail, and Nurul Aini Jaafar. "Mathematical Modeling of Unsteady Solute Dispersion in Bingham Fluid Model of Blood Flow Through an Overlapping Stenosed Artery." *Journal of Advanced Research in Fluid Mechanics and Thermal Sciences* 87, no. 3 (2021): 134-147. https://doi.org/10.37934/arfmts.87.3.134147

[75] Gudekote, Manjunatha, and Rajashekhar Choudhari. "Slip effects on peristaltic transport of Casson fluid in an inclined elastic tube with porous walls." *Journal of Advanced Research in Fluid Mechanics and Thermal Sciences* 43, no. 1 (2018): 67-80.

[76] Hamrelaine, Salim, Fateh Mebarek-Oudina, and Mohamed Rafik Sari. "Analysis of MHD Jeffery Hamel flow with suction/injection by homotopy analysis method." *Journal of Advanced Research in Fluid Mechanics and Thermal Sciences* 58, no. 2 (2019): 173-186.

[77] Kotnurkar, Asha S., and Namrata Kallolikar. "Effect of Surface Roughness and Induced Magnetic Field on Electro-Osmosis Peristaltic Flow of Eyring Powell Nanofluid in a Tapered Asymmetric Channel." *Journal of Advanced Research in Numerical Heat Transfer* 10, no. 1 (2022): 20-37.

[78] Nima, Nayema Islam, and Mohammad Ferdows. "Dual Solutions in Mixed Convection Flow Along Non-Isothermal Inclined Cylinder Containing Gyrotactic Microorganism." *Journal of Advanced Research in Fluid Mechanics and Thermal Sciences* 87, no. 3 (2021): 51-63. https://doi.org/10.37934/arfmts.87.3.5163